JACS
JOURNAL OF THE AMERICAN CHEMICAL SOCIETY

Article

pubs.acs.org/JACS

Stepwise Motion in a Multivalent [2](3)Catenane

Zheng Meng,[†,§] Ying Han,[†] Li-Na Wang,[‡] Jun-Feng Xiang,[*,‡] Sheng-Gui He,[*,‡] and Chuan-Feng Chen[*,†]

[†]Beijing National Laboratory for Molecular Sciences, CAS Key Laboratory of Molecular Recognition and Function, Institute of Chemistry, Chinese Academy of Sciences, Beijing 100190, China

[‡]Institute of Chemistry, Chinese Academy of Sciences, Beijing 100190, China

[§]University of Chinese Academy of Sciences, Beijing 100049, China

Supporting Information

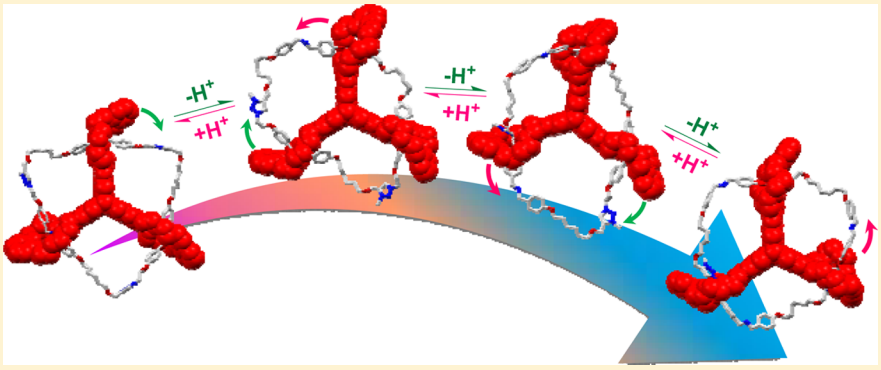

ABSTRACT: The motions of biomolecular machines are usually multistep processes, and are involved in a series of conformational changes. In this paper, a novel triply interlocked [2](3)catenane composed of a tris(crown ether) host **eTC** and a circular ditopic guest with three dibenzyl ammonium (**DBA**) sites and three *N*-methyltriazolium (**MTA**) sites was reported. Due to the multivalency nature of the catenane, the acid−base triggered motion was performed by a stepwise manner. The coconformations of the four related stable states have been directly identified and quantified which confirmed the multistep process. In order to quantify the dynamics with environmental acidity changes, the values of the three levels of dissociation constant pK_a have been determined. The special interlocked topology of the [2](3)catenane also endows the motion of each crown ether ring in the host with unexpected selectivity for the **MTA** sites. This study provides clues to comprehend the underlying motion mechanism of intricate biological molecular machines, and further design artificial molecular machine with excellent mechanochemistry properties.

INTRODUCTION

Biomolecular machines are extremely complex assemblies in cells, and they execute exquisitely controlled rotary, sliding, or walking motion governed by noncovalent interactions, to underlie their function and regulation, such as cell signaling, energy transduction, and cargo delivery.[1] These diversified motions are usually composed of multiple substeps and involved several sequential, well-defined conformational changes,[2] and usually fulfilled in a cooperative or coupled manner by their subunits.[3] During the motion of β subunit in F1-ATPase, its conformation changes from an open to a closed form upon ATP binding, providing driving force for rotation of the γ-shaft.[4] Also, at least three conformational states of myosin corresponding to different steps in the actomyosin cycle have been identified.[5] The conformational dynamics[6] of these large, intricate complexes, however, remain horrible challenges to characterize.

Since catenane- and rotaxane-based molecular machine prototypes were proposed, elementary types of motions, which are based on the interconversion between different coconformations of mechanically interlocked molecules (MIMs)[7] under proper stimulation, have already been successfully fulfilled at the molecular level.[8] Intimate knowledge of dynamic parameters of stable state coconformations can offer a key to understand mechanisms of the mechanical motion, and depict one piece of the blueprint for programming a MIM to fit the demands of a given function, such as processive catalysis,[9] information storage,[10] and directional motion.[11]

With the desire to build more elaborate nanosystems analogous to nature's examples, multivalency[12] is likely to play an increasingly significant role. Multivalent interactions offer the advantage of multiple and sequential binding[13] within the host−guest systems over the monovalent receptor−ligand interaction. The controllability of noncovalent interaction by either a chemical or physical manner suggests that the number of defined binding sites in a multivalent assembly can be variant.[14] As a result, the introduction of the multivalency

Received: June 10, 2015
Published: July 17, 2015

DOI: 10.1021/jacs.5b05758
J. Am. Chem. Soc. 2015, 137, 9739−9745

Scheme 1. (a) Synthetic Route to the Pyrazine-Extended Triptycene-Based Tris(crown ether) Host eTC, (b) Single Crystal Structure of eTC, and (c) Synthesis of the [2](3)Catenane C-H_3·6PF_6 and the Labels of Protons

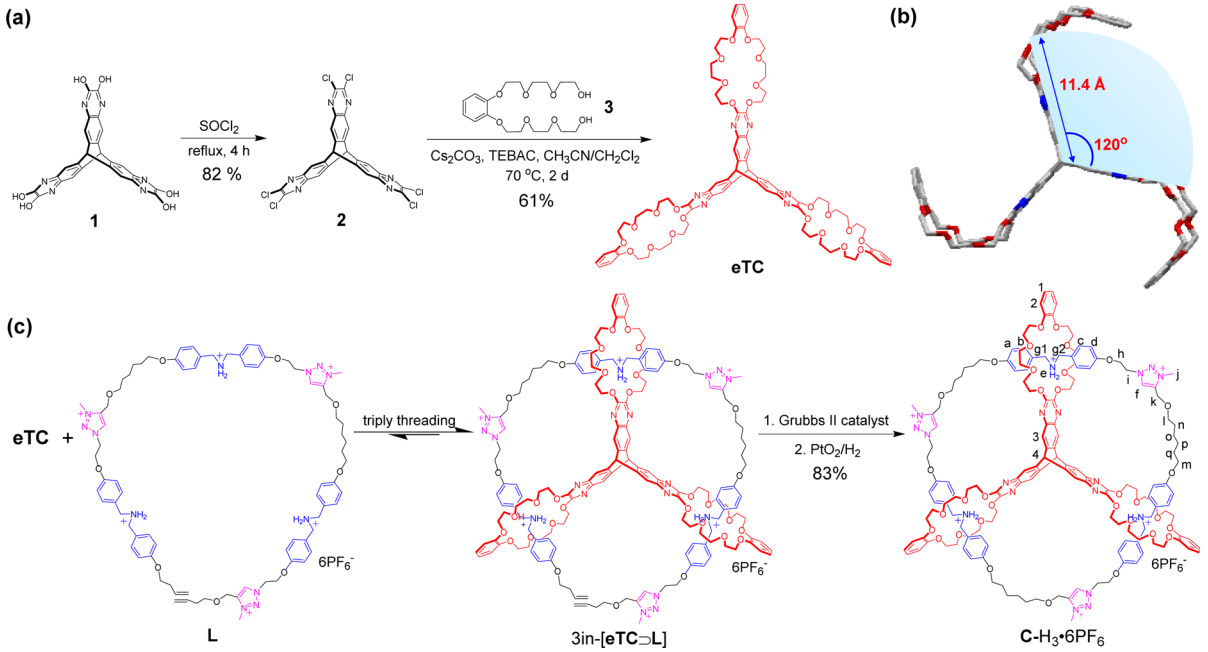

concept into a switchable artificial system may allow us to break up the whole molecular motion into several parts by forming partly binding conformations.[15] Excavating the details in complex molecular motion is thus feasible. However, studies about the switchable MIM systems that benefit from multivalency are rare.[16]

In this paper, we report the synthesis, structure, and motion mechanism of a novel triply interlocked[17] [2](3)catenane C-H_3·6PF_6 featuring a pyrazine-extended triptycene-derived tris(crown ether) host **eTC** triply penetrated by a circular ditopic guest with three **DBA** sites and three **MTA**[18] sites. The multivalency nature of the catenane rendered a stepwise motion by gradually destroying the **DBA**-crown ether interaction and facilitating the **MTA**-crown ether interaction during its three-step deprotonation process. This multistep process was unambiguously confirmed by identifying and quantifying the coconformations of the four stable states. To evaluate the thermodynamic feature with the acidity change in environment, the values of the three levels of dissociation constant pK_a of C-H_3·6PF_6 were measured by an indicator method. Moreover, due to the special interlocked structure of the [2](3)catenane, after each deprotonation of the **DBA** group, one crown ether ring of the host preferentially resided on one of two **MTA** sites with closer distance to form a more stable coconformation. This selectivity for sites generally without discriminating affinities is unprecedented in known MIM systems.

RESULTS AND DISCUSSION

Molecular Design and Synthesis. Our group has previously reported a D_{3h} symmetrical triptycene tris(crown ether) host.[19] Its three dibenzo-24-crown-8 (DB24C8) rings are positioned in three orientations, which not only allow three dibenzylammonium guests to thread in, but also can accommodate a bent linear trisdialkylammonium strand to facilitate highly efficient synthesis of a [4]pseudocatenane.[20] To introduce more recognition stations into the guest component for the construction of functional catenanes, we proposed that a host with more free volume between the adjacent DB24C8 rings would better meet the requirement of the steric hindrance. Thus, a pyrazine-extended triptycene-derived tris(crown ether) host **eTC** was designed. Hexahydroxytriptycene **1** was subjected in thionyl chloride to give hexachlorotriptycene **2**. Then the reaction of **2** with diol **3** under the presence of Cs_2CO_3 using benzyltriethylammonium chloride (TEBAC) as catalyst generated the product **eTC** in a satisfying isolated yield of 61% (Scheme 1a). The single crystal structure of **eTC** shows that a D_{3h} symmetrical conformation was adopted in the solid state, and a 120° fan shaped zone with r = 11.4 Å was wedged between the adjacent benzo-24-crown-8 (B24C8) rings (Scheme 1b).

Having grasped the structural features of host **eTC**, we further designed and synthesized the linear guest **L** with two alkenyl ends by a modular splicing strategy (see Supporting Information for details). Three **DBA** and **MTA** recognition sites for DB24C8 are regularly aligned in **L**. The complexation between host **eTC** and guest strand **L** was then investigated in solution. The ^{1}H NMR spectrum (see Figure S1 in Supporting Information) of the equimolar mixture of **eTC** and **L** in a solvent of CD_2Cl_2/acetone-d_6 (v/v = 2:1) showed that the formation of the desired triply interlocked pseudorotaxane 3in-[**eTC**⊃**L**] was rather complete. Treatment of the mixture in CH_2Cl_2/acetone (v/v = 2:1, 1.0 mM) with a catalytic amount of Grubbs second-generation catalyst at 45 °C for 48 h resulted in the [2](3)catenane in a reasonably high yield of 83% after hydrogenation and purification (Scheme 1c). This high yield should be attributed to the good efficiency of multivalency directed self-assembly and the dynamic ring-closing olefin metathesis allowing the formation of the thermodynamically stable product by error correction.

Structure Characterization and Acid−Base Triggered Molecular Switching. The concise ^{1}H NMR spectra (Figure 1a and Figure S2 in Supporting Information) of C-H_3·6PF_6 indicated that an averaged D_{3h} symmetrical coconformation was adopted in solution. By utilizing COSY, HSQC, and ROESY

DOI: 10.1021/jacs.5b05758
J. Am. Chem. Soc. 2015, 137, 9739−9745

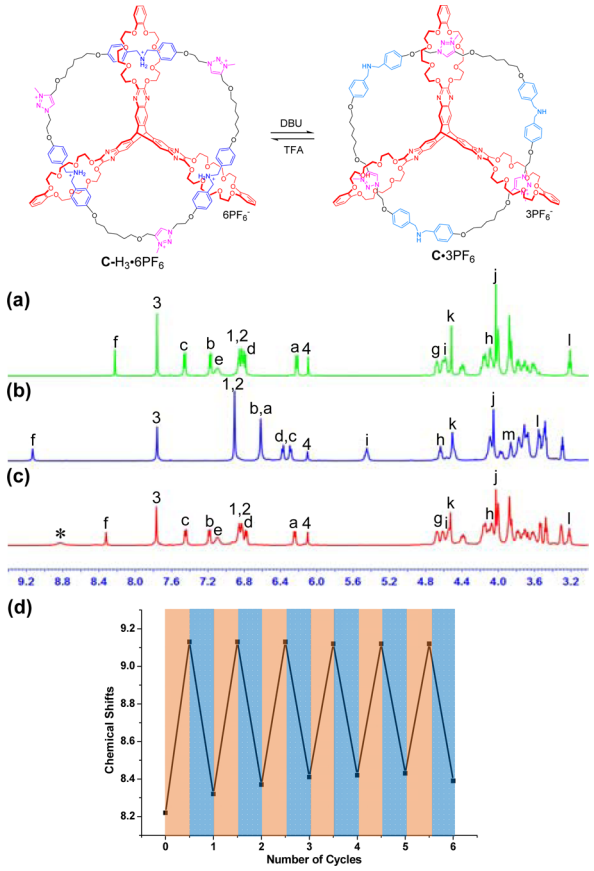

Figure 1. Partial ^{1}H NMR spectra (500 MHz, 298 K, CD_3CN, c = 4.0 mM) of (a) **C**-H_3·6PF_6; (b) the solution obtained after adding 3.2 equiv of DBU to **C**-H_3·6PF_6; (c) the solution obtained after adding 3.4 equiv of TFA to the solution in part (b). * denotes TFA. (d) Acid–base switching of [2](3)catenane **C**-H_3·6PF_6 monitored by ^{1}H NMR spectroscopy. The chemical shifts of H_f were recorded.

experiments, the vast majority of the ^{1}H signals have been assigned (Supporting Information Figures S4–S6). In **C**-H_3·6PF_6, all the three crown ether rings preferentially resided on the **DBA** sites because they have higher affinities with the crown ether ring than **MTA** sites. The ROESY spectrum (Figure S6 in Supporting Information) gave clear cross peaks of H_b, H_c, and ethylene glycol protons, providing direct evidence for the interactions between **DBA** sites and B24C8 rings. The **MTA** sites located at one side of the B24C8 rings are nearly six atoms further from the bound **DBA** sites than those at the other side. After the **DBA** sites were deprotonated by 3.2 equiv of 1,8-diazabicyclo[5.4.0]undec-7-ene (DBU), all of the crown ether rings migrated to **MTA** sites to produce the catenane **C**·3PF_6, which could be isolated and purified by simple procedure in 91% yield (see Supporting Information). As shown in Figure 1b, the resonances of protons H_f were shifted significantly downfield with a $\Delta\delta$ = 0.91 ppm, as a consequence of interaction of **MTA** recognition site with the B24C8 ring which were further affirmed by the ROESY spectrum. Like **C**-H_3·6PF_6, **C**·3PF_6 also has a highly symmetrical coconformation in solution revealed by the ^{1}H NMR spectrum. Further addition of a slight excess (3.4 equiv) of trifluoroacetic acid (TFA) restored the location of the crown ether rings to **DBA** sites (Figure 1c). The clear-cut reversible acid–base triggered switching between **C**-H_3·6PF_6 and **C**·3PF_6 went smoothly with efficiency degradation <25% after 6 complete cycles, as proved by ^{1}H NMR spectroscopic investigations (Figure 1d and Supporting Information Figure S14).

Stepwise Molecular Motion. The presence of multiple nondegenerate recognition sites in **C**-H_3·6PF_6 inspired us to consider whether the coconformations, in which one or two crown ether rings binds to **DBA** site(s) and the rest to **MTA** site(s), would appear during the acid–base triggered switching (Figure 2a). Elucidating the dynamics of these coconformations will undoubtedly provide fundamental information for uncovering the motion mechanism. Consequently, a series of titration experiments were performed. It was found that the continuous addition of DBU (<3.0 equiv) to **C**-H_3·6PF_6 resulted in very complicated ^{1}H NMR spectra (Supporting Information Figure S16a), which is a sign of the coexistence of different coconformations due to the incomplete deprotonation of **DBA** sites. Interestingly, the chemical shifts of protons H_f were found to be single peaks and clearly resolved, which could thus provide ideal probes to trace the whole evolution process. In **C**-H_3·6PF_6 or **C**·3PF_6, the protons H_f showed only a single peak at a relative upfield of 8.22 ppm and a relative downfield of 9.13 ppm, respectively. With the addition of <0.5 equiv of DBU, one set of H_f signals with three peaks, one at the relative downfield and two at the relative upfield, gradually emerged in a integral ratio of 1:1:1 (Figure 2b). This implied that, after the deprotonation of one **DBA** group, the species **C**-H_2·5PF_6 which has a coconformation with one of the three crown ether rings binding at **MTA** sites generated. The subsequent addition of DBU (>0.75 equiv) generated another new set of H_f signals with three peaks, still in a ratio of 1:1:1; however, two were at the relative downfield and one at the relative upfield. Thus, a coconformation with two crown ether rings surrounding the **MTA** sites could be easily deduced for **C**-H_1·4PF_6. The sequential content changes of different species in **C**-H_3·6PF_6 solution upon the addition of DBU were also reflected in the fluorescent spectrum, although the absorbance of **C**-H_3·6PF_6 and **C**·3PF_6 showed only negligible difference (Figure 2d). Obvious emission quenching at 369 nm was observed upon the addition of DBU to **C**-H_3·6PF_6, which might have resulted from a photoinduced electron transfer effect between the dibenzylamine electron donor and the quinoxaline fluorophore.[21] Fluorometric titrations depicted in Figure 2e showed that the fluorescence intensity was steadily decreased to 20% of the initial by the addition of DBU to 3.2 equiv, while nearly 3-fold fluorescence enhancement was finally obtained upon the titration of TFA to **C**·3PF_6 (Figure 2f).

The contents of the four species **C**-H_3·6PF_6, **C**-H_2·5PF_6, **C**-H_1·4PF_6, and **C**·3PF_6 could be easily quantified by integration of H_f signals in ^{1}H NMR spectra. As shown in Figure 2c, the addition of 1 or 2 equiv of base to **C**-H_3·6PF_6 did not exclusively lead to **C**-H_2·5PF_6 or **C**-H_1·4PF_6, but mixtures of differently deprotonated species. This phenomenon is a consequence of the ternary Brønsted acid characteristic of **C**-H_3·6PF_6. Distributions of the four species were determined by the amount of the base added (the acidity of the environment) and the three levels of dissociation constants (K_a).

Considering their Brønsted acid or base nature, for any acid–base triggered molecular switch or machine with definite chemical structure, pK_a should be a critically important parameter to quantitatively judge its acidic (basic) strength and dynamic under the environment of different acidities. However, at present no acid–base switchable MIM systems[22] have given the related thermodynamic constants. We found that the methyl red with pK_a of 10.2 in acetonitrile[23] could be a

DOI: 10.1021/jacs.5b05758
J. Am. Chem. Soc. 2015, 137, 9739–9745

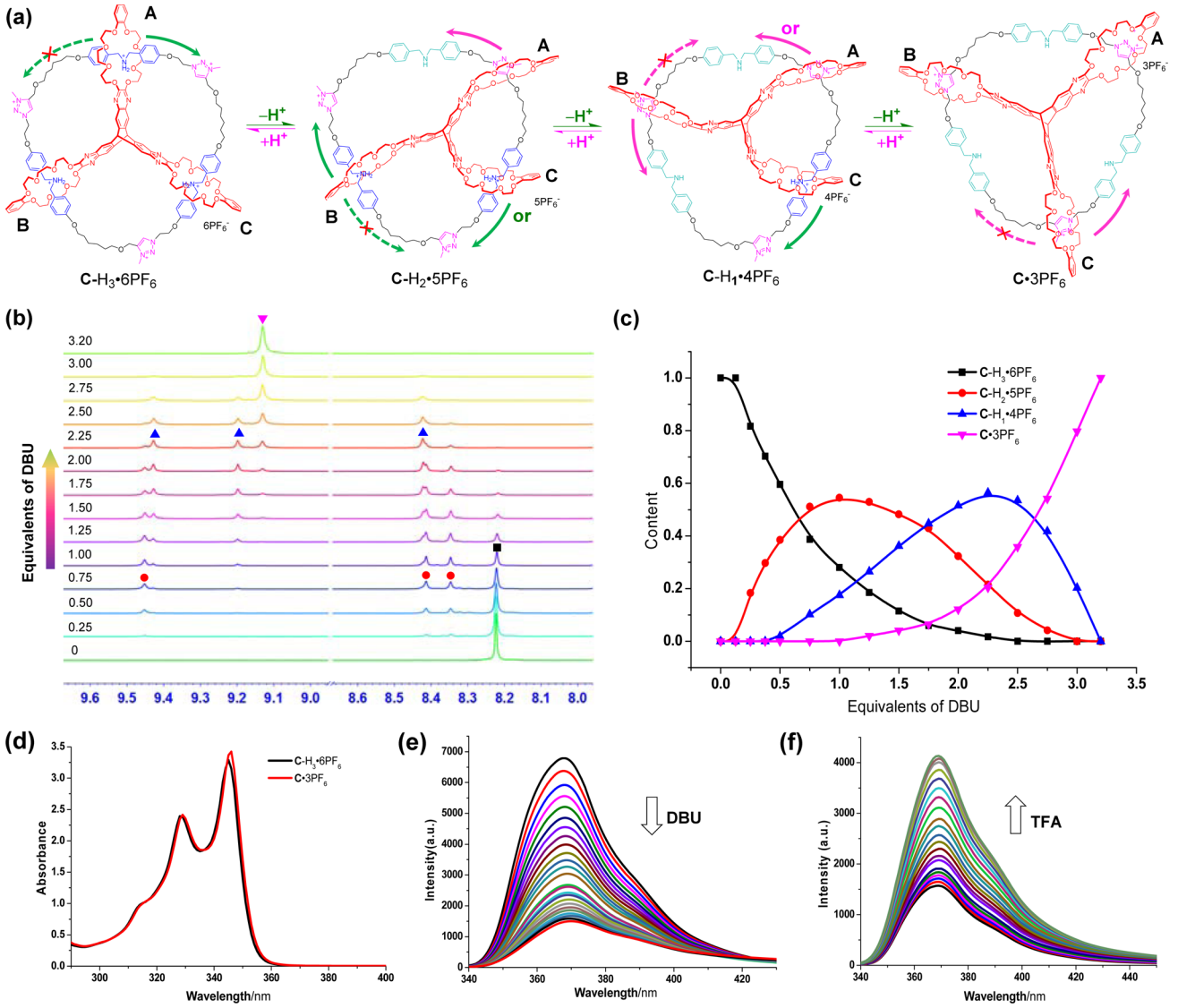

Figure 2. (a) Scheme representation of the acid–base triggered motion. The three crown ether rings are labeled with A, B, and C for the convenience of discussion. After the catenanes were triggered by acid or base, thermodynamically favorable pathways for B24C8 rings of the host molecule are designated arrows with green or pink color, respectively. (b) ^{1}H NMR spectra (500 MHz, 298 K, CD_3CN, $c = 4.0 \times 10^{-3}$ M) for **MTA** aromatic protons (H_f) of **C**-H_3·$6PF_6$ (■), **C**-H_2·$5PF_6$ (●), **C**-H_1·$4PF_6$ (▲), and **C**·$3PF_6$ (▼) during the titration. (c) Distributions of the four species versus the amount of DBU added. (d) UV–vis absorption of **C**-H_3·$6PF_6$ and **C**·$3PF_6$ recorded in MeCN ($c = 4.0 \times 10^{-5}$ M). The fluorescence spectral changes upon (e) the successive addition of DUB to a solution of **C**-H_3·$6PF_6$ in MeCN, and (f) the successive addition of TFA to a solution of **C**·$3PF_6$ in MeCN ($c = 4.0 \times 10^{-5}$ M, $\lambda_{ex} = 335$ nm, $\lambda_{em} = 369$ nm).

proper indicator to monitor the acidity change in the UV–vis titration experiments. Thus, with a combination of the above NMR titration results under the same condition, the pK_{a1}, pK_{a2}, and pK_{a3} values of **C**-H_3·$6PF_6$ could be calculated by the following equation (see Supporting Information for details):

$$pK_{an} = pK_{HIn} - \log\frac{[HIn]}{[In^-]} + \log\frac{\{[\mathbf{C}\text{-}H_{3-n+1}]^{(6-n+1)+}\}}{\{[\mathbf{C}\text{-}H_{3-n}]^{(6-n)+}\}}$$

$$n = 1, 2, 3$$

In this equation, $[HIn]/[In^-]$ is the concentration ratio of the acid and base form of the indicator, calculated from the UV–vis titration results. The ratios of the conjugate acid–base pairs of the four species were figured out by the NMR titrations (Figure 2c). According to the equation, the pK_a values with good precision up to ±0.2 pK_a units were obtained, and listed in Table 1. The $\Delta pK_{a1,2}$, $\Delta pK_{a2,3}$, $\Delta pK_{a1,3}$ values were 0.57, 0.98, and 1.55, respectively, implying that non-negligible divergences of the ionization abilities of the three **DBA** sites existed. Although the ΔpK_a values were not large enough to form discrete partly deprotonated spieces (**C**-H_2·$5PF_6$ and **C**-H_1·

Table 1. Thermodynamic Data of Dissociation Equilibria for C-H_3·$6PF_6$ at 298 K in Acetonitrile

equilibrium	pK_a	ΔG/(kJ mol^{-1})[a]
$[\mathbf{C}\text{-}H_3]^{6+} \rightleftharpoons [\mathbf{C}\text{-}H_2]^{5+} + H^+$	9.78 ± 0.16	55.8 ± 0.9
$[\mathbf{C}\text{-}H_2]^{5+} \rightleftharpoons [\mathbf{C}\text{-}H_1]^{4+} + H^+$	10.35 ± 0.05	59.0 ± 0.3
$[\mathbf{C}\text{-}H_1]^{4+} \rightleftharpoons [\mathbf{C}]^{3+} + H^+$	11.33 ± 0.10	64.6 ± 0.6

[a]The free energies of dissociation (ΔG) were calculated from the K_a values by using the expression $\Delta G = -RT \ln K_a$.

DOI: 10.1021/jacs.5b05758
J. Am. Chem. Soc. 2015, 137, 9739–9745

$4PF_6$) in acetonitrile, the whole switching process was still performed in a palpable order. The present data also suggested in theory that bases such as tributylamine and 1,4-diazabicyclo-[2,2,2]octane may be suitable chemical sources to drive the molecular motion of catenane **C**-H_3·$6PF_6$ and the related **MIM** systems, but 2,6-lutidine, quinuclinide, and *N*-ethyldiisopropyl-amine do not work.[24]

The above results illustrated that the motion of the three crown ether rings from **DBA** to **MTA** sites after the addition of base was in a stepwise manner (Figure 2a). With the deprotonation of the **DBA** sites, one of three crown ether rings in **C**-H_3·$6PF_6$ began to move to the **MTA** site, then two, and finally all three rings reached the **MTA** sites. The ^{1}H NMR titration experiments pointed out that reverse acid triggered motion starting from **C**·$3PF_6$ also followed a stepwise fashion (see Supporting Information Figure S19).

Selectivity in the Stepwise Motion. Theoretically speaking, after deprotonation of one **DBA** group in **C**-H_3·$6PF_6$, B24C8 ring A may choose one of the two possible paths to occupy either the nearer or the further **MTA** site to produce **C**-H_2·$5PF_6$, or quickly oscillate between the two quasidegenerate **MTA** sites. In the next step, either the **DBA** site binding to ring B or ring C in **C**-H_2·$5PF_6$ may be deprotonated, causing the corresponding ring to migrate. Considering the equivalent situation involved, these two circumstances could be simplified as discussing ring B's possible locations in **C**-H_1·$4PF_6$.

We first turned to variable-temperature (VT) ^{1}H NMR spectroscopy to evaluate the dynamics of **C**-H_2·$5PF_6$ and **C**-H_1·$4PF_6$. Even though the temperatures have been raised to 348 K, no significant changes were observed for all the proton signals of **C**-H_2·$5PF_6$ and **C**-H_1·$4PF_6$ (see Supporting Information Figures S21, S22), indicating their relatively stable coconformations within the range of tested temperatures. Importantly, there is no trend of the coalescence of H_f in different regions for both of them as shown in Figure 3. This is quite different from that in a degenerate [2]rotaxane, whose aromatic proton signals of two **MTA** sites coalesced at 338 K in CD_3CN because of the DB24C8 ring's rapid vibration.[25] The lack of coalescence indicated that in **C**-H_2·$5PF_6$ the crown ether ring A (ring B for **C**-H_1·$4PF_6$) had special dynamic features, and was inclined to sit on one of the two **MTA** sites beside the newly generated dibenzylamine group. Nevertheless, it seems to be counter-intuitive considering that the two **MTA** groups have no discriminating affinities for the crown ether ring.

Calculations based on B3LYP/3-21G were then carried out to gain further insights into stabilities and structural characteristics of the four species. As depicted in Figure 4, both **C**-H3·$6PF_6$ and **C**·$3PF_6$ adopted pseudo-D_{3h} symmetrical coconformation. For the two possible coconformations of **C**-H_2·$5PF_6$ (Figure 4b) and **C**-H_1·$4PF_6$ (Figure 4c), the coconformers i were more favorable by 4.8, 18.0[26] kcal mol^{-1} than coconformers ii, respectively. On the basis of the Boltzmann distribution law, distribution ratios for the coconformers i and ii were much higher than 1000:1 at 298 K. For the less stable coconformations ii, both of the host and guest components possessed very distorted structures, which should cause considerable enthalpy loss. In the coconformer i of **C**-H_2·$5PF_6$ or **C**-H_1·$4PF_6$, a C6 linker (Figure 2a) was clamped by B24C8 ring A and C with very close distance. It coincides with their ^{1}H NMR spectroscopy in which the signals of the protons $H_{o,p,q}$ are all at higher frequencies (see Supporting Information Figure S16d) compared with those of **C**-H_3·$6PF_6$ and **C**·$3PF_6$ due to the shielding effect of the two B24C8 rings.

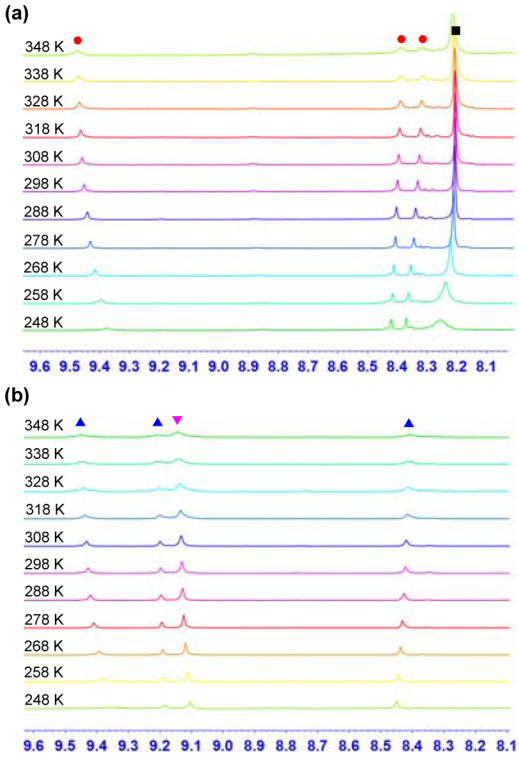

Figure 3. VT ^{1}H NMR spectra (500 MHz, CD_3CN, c = 4.0 mM) for H_f after the addition of 0.5 (a) and 2.5 (b) equiv of DBU in **C**-H_3·$6PF_6$. The labels are the same as those in Figure 2b.

In sharp contrast to [2]rotaxane analogues with linear structure, the parts of the guest between two B24C8 rings of these four species are seriously bent due to the structural restrictions from the host molecule. Meanwhile, because the three crown ether rings are covalently linked by the rigid triptycene core, the freedom for one B24C8 ring's migration on the guest component is limited when the other two rings are tethered by the recognition sites. Due to these mutual influences of the topologically linked components, oscillation of ring A between the two **MTA** sites was very likely prohibited when one of the **DBA** site was deprotonated in **C**-H_3·$6PF_6$. Similarly, ring B's shuttling in **C**-H_1·$4PF_6$ was also extremely stunted. That is why, even at 348 K, we could not observe any trend of the coalescence of H_f signals. The binding of the B24C8 ring at the closer **MTA** site (**C**-H_3·$6PF_6$ → **C**-H_2·$5PF_6$-i or **C**-H_2·$5PF_6$-i → **C**-H_1·$4PF_6$-i) beside the deprotonated **DBA** group did not involve such a large amplitude coconformational adjustment of the whole interlocked structure as binding at the further one (**C**-H_3·$6PF_6$ → **C**-H_2·$5PF_6$-ii or **C**-H_2·$5PF_6$-i → **C**-H_1·$4PF_6$-ii), which presaged a much faster kinetic for the former.

CONCLUSIONS

In this work, we have demonstrated the design and highly efficient synthesis of a novel two-component, triply interlocked [2](3)catenane **C**-H_3·$6PF_6$ using a pyrazine-extended triptycene-derived tris(crown ether) host **eTC** by a dynamic covalent chemistry approach.[27] The nondegenerate multivalent interactions in the catenane allow us to gradually destroy or restore one of the two modes of intercations by acid−base stimuli. Thus, a controlled stepwise motion was generated, which has been simply and definitely confirmed with the four stable states identified and quantified by the ^{1}H NMR titration experiments.

DOI: 10.1021/jacs.5b05758
J. Am. Chem. Soc. 2015, 137, 9739−9745

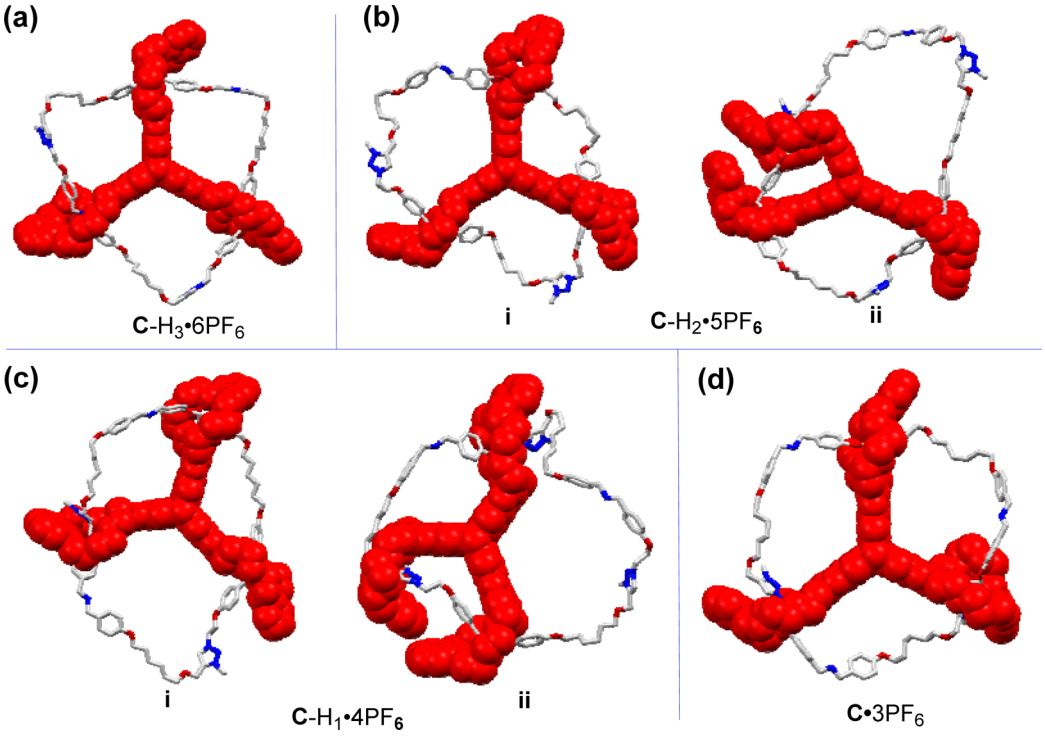

Figure 4. Structures of **C**-H_3·$6PF_6$ (a) and **C**·$3PF_6$ (d) and the two possible stable coconformations of **C**-H_2·$5PF_6$ (b) and **C**-H_1·$4PF_6$ (c) optimized by B3LYP/3-21G. All other hydrogen atoms have been removed for clarity.

By an indicator method, we for the first time determined thermodynamic data (pK_a) of dissociation equilibria for an acid−base switchable MIM system, which made a quantitative and accurate estimate for its dynamic with environmental acidity change become practicable.

Harnessing the multivalency, we have drawn a clear picture of the motion mechanism at the present MIM system by elucidating the stepwise coconformational evolution through NMR techniques and quantum chemistry calculations. After the deprotonation of **DBA** sites, the so-liberated rings preferentially moved to the spatially closer **MTA** sites to form thermodynamically stable coconformations rather than migrating to the further ones, in a clockwise or counterclockwise sequence. The selectivity is exotic because a single DB24C8 ring would show no discriminating recognition abilities for the two **MTA** sites. This phenomenon indicated that a fundamental relationship exists between structure topology and mechanical properties.[7b,28]

As all the experimental and calculated data implied that the paths of the B24C8 ring to nearer recognition sites are also probably kinetically favorable, by introducing other functional spacer in the [2](3)catenane,[29] an all-around mechanostereoselectivity[30] control would be realized to fulfill unidirectional 360° rotation. The present system thus laid a foundation for constructing molecular motors[31] with superior structural and mechanical properties. Our study also provides enlightenment to understand the operation mechanism of the intricate biological molecular machines, for example, the proton gradient powered rotary motion of ATP synthase.

■ ASSOCIATED CONTENT

Supporting Information

Detailed synthesis, characterization data of all the new compounds, additional experimental results, and single crystal data, including data in CIF format. The Supporting Information is available free of charge on the ACS Publications website at DOI: 10.1021/jacs.5b05758.

■ AUTHOR INFORMATION

Corresponding Authors

cchen@iccas.ac.cn
shengguihe@iccas.ac.cn
jfxiang@iccas.ac.cn

Notes

The authors declare no competing financial interest.

■ ACKNOWLEDGMENTS

We thank the National Natural Science Foundation of China (21332008, 91127009, and 51373180), the National Basic Research Program (2011CB932501), and the Strategic Priority Research Program of the Chinese Academy of Sciences (XDB12010400) for financial support.

■ REFERENCES

(1) Frank, J. *Molecular Machines in Biology: Workshop of the Cell*; Cambridge University Press: New York, 2011.
(2) Schliwa, M.; Woehlke, G. *Nature* **2003**, *422*, 759.
(3) Ning, W.; Fei, J.; Gonzalez, R. L., Jr. *Proc. Natl. Acad. Sci. U. S. A.* **2014**, *111*, 12073.
(4) (a) Ito, Y.; Oroguchi, T.; Ikeguchi, M. *J. Am. Chem. Soc.* **2011**, *133*, 3372−3380. (b) Czub, J.; Grubmuller, H. *J. Am. Chem. Soc.* **2014**, *136*, 6960.
(5) Houdusse, A.; Szent-Gyorgyi, A. G.; Cohen, C. *Proc. Natl. Acad. Sci. U. S. A.* **2000**, *97*, 11238.
(6) (a) Weiss, S. *Nat. Struct. Biol.* **2000**, *7*, 724. (b) Pan, Y.; Brown, L.; Konermann, L. *J. Am. Chem. Soc.* **2011**, *133*, 20237.
(7) (a) Sauvage, J. P.; Dietrich-Buchecker, C. *Catenanes, Rotaxanes, and Knots*; Wiley-VCH: Weinheim, Germany, 1999. (b) van Dongen, S. F.; Cantekin, S.; Elemans, J. A.; Rowan, A. E.; Nolte, R. J. *Chem. Soc.*

DOI: 10.1021/jacs.5b05758
J. Am. Chem. Soc. 2015, 137, 9739−9745

Rev. **2014**, *43*, 99. (c) Xue, M.; Yang, Y.; Chi, X.; Yan, X.; Huang, F. *Chem. Rev.* **2015**, DOI: 10.1021/cr5005869. (d) Gil-Ramirez, G.; Leigh, D. A.; Stephens, A. J. *Angew. Chem., Int. Ed.* **2015**, *54*, 6110.
(8) (a) Kay, E. R.; Leigh, D. A.; Zerbetto, F. *Angew. Chem., Int. Ed.* **2007**, *46*, 72. (b) Balzani, V.; Credi, A.; Venturi, M. *Molecular Devices and Machines: Concepts and Perspectives for the Nanoworld*, 2nd ed.; Wiley-VCH: Weinheim, Germany, 2008.
(9) (a) Thordarson, P.; Bijsterveld, E. J.; Rowan, A. E.; Nolte, R. J. *Nature* **2003**, *424*, 915. (b) Lewandowski, B.; De Bo, G.; Ward, J. W.; Papmeyer, M.; Kuschel, S.; Aldegunde, M. J.; Gramlich, P. M.; Heckmann, D.; Goldup, S. M.; D'Souza, D. M.; Fernandes, A. E.; Leigh, D. A. *Science* **2013**, *339*, 189.
(10) Green, J. E.; Choi, J. W.; Boukai, A.; Bunimovich, Y.; Johnston-Halperin, E.; DeIonno, E.; Luo, Y.; Sheriff, B. A.; Xu, K.; Shin, Y. S.; Tseng, H. R.; Stoddart, J. F.; Heath, J. R. *Nature* **2007**, *445*, 414.
(11) (a) Leigh, D. A.; Wong, J. K.; Dehez, F.; Zerbetto, F. *Nature* **2003**, *424*, 174. (b) Ragazzon, G.; Baroncini, M.; Silvi, S.; Venturi, M.; Credi, A. *Nat. Nanotechnol.* **2015**, *10*, 70.
(12) Fasting, C.; Schalley, C. A.; Weber, M.; Seitz, O.; Hecht, S.; Koksch, B.; Dernedde, J.; Graf, C.; Knapp, E. W.; Haag, R. *Angew. Chem., Int. Ed.* **2012**, *51*, 10472.
(13) (a) Hess, V. L.; Szabo, A. *J. Chem. Educ.* **1979**, *56*, 289. (b) Badjic, J. D.; Cantrill, S. J.; Stoddart, J. F. *J. Am. Chem. Soc.* **2004**, *126*, 2288. (c) Jiang, W.; Nowosinski, K.; Low, N. L.; Dzyuba, E. V.; Klautzsch, F.; Schafer, A.; Huuskonen, J.; Rissanen, K.; Schalley, C. A. *J. Am. Chem. Soc.* **2012**, *134*, 1860.
(14) Badjic, J. D.; Nelson, A.; Cantrill, S. J.; Turnbull, W. B.; Stoddart, J. F. *Acc. Chem. Res.* **2005**, *38*, 723.
(15) (a) Lund, K.; Manzo, A. J.; Dabby, N.; Michelotti, N.; Johnson-Buck, A.; Nangreave, J.; Taylor, S.; Pei, R.; Stojanovic, M. N.; Walter, N. G.; Winfree, E.; Yan, H. *Nature* **2010**, *465*, 206. (b) Perl, A.; Gomez-Casado, A.; Thompson, D.; Dam, H. H.; Jonkheijm, P.; Reinhoudt, D. N.; Huskens, J. *Nat. Chem.* **2011**, *3*, 317. (c) Liu, S.; Kondratuk, D. V.; Rousseaux, S. A.; Gil-Ramirez, G.; O'Sullivan, M. C.; Cremers, J.; Claridge, T. D.; Anderson, H. L. *Angew. Chem., Int. Ed.* **2015**, *54*, 5355.
(16) (a) Balzani, V.; Clemente-Leon, M.; Credi, A.; Lowe, J. N.; Badjic, J. D.; Stoddart, J. F.; Williams, D. J. *Chem. - Eur. J.* **2003**, *9*, 5348. (b) Badjic, J. D.; Balzani, V.; Credi, A.; Silvi, S.; Stoddart, J. F. *Science* **2004**, *303*, 1845. (c) Zhang, Z.-J.; Han, M.; Zhang, H.-Y.; Liu, Y. *Org. Lett.* **2013**, *15*, 1698.
(17) (a) Fujita, M.; Fujita, N.; Ogura, K.; Yamaguchi, K. *Nature* **1999**, *400*, 52. (b) Westcott, A.; Fisher, J.; Harding, L. P.; Rizkallah, P.; Hardie, M. J. *J. Am. Chem. Soc.* **2008**, *130*, 2950. (c) Fukuda, M.; Sekiya, R.; Kuroda, R. *Angew. Chem., Int. Ed.* **2008**, *47*, 706. (d) Li, Y.; Mullen, K. M.; Claridge, T. D.; Costa, P. J.; Felix, V.; Beer, P. D. *Chem. Commun.* **2009**, 7134. (e) Hasell, T.; Wu, X.; Jones, J. T.; Bacsa, J.; Steiner, A.; Mitra, T.; Trewin, A.; Adams, D. J.; Cooper, A. I. *Nat. Chem.* **2010**, *2*, 750. (f) Bar, A. K.; Raghothama, S.; Moon, D.; Mukherjee, P. S. *Chem. - Eur. J.* **2012**, *18*, 3199. (g) Pun, A.; Hanifi, D. A.; Kiel, G.; O'Brien, E.; Liu, Y. *Angew. Chem., Int. Ed.* **2012**, *51*, 13119. (h) Meng, Z.; Chen, C.-F. *Chem. Commun.* **2015**, *51*, 8241.
(18) Coutrot, F.; Busseron, E. *Chem. - Eur. J.* **2008**, *14*, 4784.
(19) Zhu, X.-Z.; Chen, C.-F. *J. Am. Chem. Soc.* **2005**, *127*, 13158.
(20) Jiang, Y.; Zhu, X.-Z.; Chen, C.-F. *Chem. - Eur. J.* **2010**, *16*, 14285.
(21) Mandal, A. K.; Gangopadhyay, M.; Das, A. *Chem. Soc. Rev.* **2015**, *44*, 663.
(22) (a) Ashton, P. R.; Ballardini, R.; Balzani, V.; Baxter, I.; Credi, A.; Fyfe, M. C. T.; Gandolfi, M. T.; Gomez-Lopez, M.; Martinez-Diaz, M. V.; Piersanti, A.; Spencer, N.; Stoddart, J. F.; Venturi, M.; White, A. J. P.; Williams, D. J. *J. Am. Chem. Soc.* **1998**, *120*, 11932. (b) Elizarov, A. M.; Chiu, S.-H.; Stoddart, J. F. *J. Org. Chem.* **2002**, *67*, 9175. (c) Tuncel, D.; Ozsar, O.; Tiftik, H. B.; Salih, B. *Chem. Commun.* **2007**, 1369. (d) Fang, L.; Hmadeh, M.; Wu, J.; Olson, M. A.; Spruell, J. M.; Trabolsi, A.; Yang, Y.-W.; Elhabiri, M.; Albrecht-Gary, A.-M.; Stoddart, J. F. *J. Am. Chem. Soc.* **2009**, *131*, 7126. (e) Grunder, S.; McGrier, P. L.; Whalley, A. C.; Boyle, M. M.; Stern, C.; Stoddart, J. F. *J. Am. Chem. Soc.* **2013**, *135*, 17691.
(23) (a) Kolthoff, I. M.; Chantooni, M. K.; Bhowmik, S. *Anal. Chem.* **1967**, *39*, 315−320. (b) Blackwell, L. F.; Fischer, A.; Miller, I. J.; Topsom, R. D.; Vaughan, J. *J. Chem. Soc.* **1964**, 3588.
(24) Badjic, J. D.; Ronconi, C. M.; Stoddart, J. F.; Balzani, V.; Silvi, S.; Credi, A. *J. Am. Chem. Soc.* **2006**, *128*, 1489.
(25) Blanco, V.; Carlone, A.; Hanni, K. D.; Leigh, D. A.; Lewandowski, B. *Angew. Chem., Int. Ed.* **2012**, *51*, 5166.
(26) When the calculations were performed by polarizable continuum model (PCM) with acetonitrile as a solvent, the corresponding energy differences were 4.0 and 12.2 kcal mol^{-1}, respectively.
(27) (a) Haussmann, P. C.; Stoddart, J. F. *Chem. Rec.* **2009**, *9*, 136. (b) Jin, Y.; Yu, C.; Denman, R. J.; Zhang, W. *Chem. Soc. Rev.* **2013**, *42*, 6634.
(28) Frasconi, M.; Kikuchi, T.; Cao, D.; Wu, Y.; Liu, W. G.; Dyar, S. M.; Barin, G.; Sarjeant, A. A.; Stern, C. L.; Carmieli, R.; Wang, C.; Wasielewski, M. R.; Goddard, W. A., III; Stoddart, J. F. *J. Am. Chem. Soc.* **2014**, *136*, 11011.
(29) Baroncini, M.; Silvi, S.; Venturi, M.; Credi, A. *Angew. Chem., Int. Ed.* **2012**, *51*, 4223.
(30) Fahrenbach, A. C.; Bruns, C. J.; Li, H.; Trabolsi, A.; Coskun, A.; Stoddart, J. F. *Acc. Chem. Res.* **2014**, *47*, 482.
(31) (a) Hernandez, J. V.; Kay, E. R.; Leigh, D. A. *Science* **2004**, *306*, 1532. (b) von Delius, M.; Geertsema, E. M.; Leigh, D. A. *Nat. Chem.* **2010**, *2*, 96. (c) Cheng, C.; McGonigal, P. R.; Schneebeli, S. T.; Li, H.; Vermeulen, N. A.; Ke, C.; Stoddart, J. F. *Nat. Nanotechnol.* **2015**, *10*, 547.

DOI: 10.1021/jacs.5b05758
J. Am. Chem. Soc. 2015, 137, 9739−9745